TITLE: Predicting the individual hydraulic performance of sewer pipes in the context of climate change

AUTHORS: Hind El-Housni[1], Sophie Duchesne[2]*, and Alain Mailhot[3]

[1] Ph.D. candidate, Eau Terre Environnement Research Centre, Institut National de la recherche scientifique (INRS), 490 de la Couronne, Quebec, QC, G1K 9A9, Canada, hind.el_housni@ete.inrs.ca

[2] Ph.D., Professor, Eau Terre Environnement Research Centre, Institut National de la recherche scientifique (INRS), 490 de la Couronne, Quebec, QC, G1K 9A9, Canada, sophie.duchesne@ete.inrs.ca

[3] Ph.D, Professor, Eau Terre Environnement Research Centre, Institut National de la recherche scientifique (INRS), 490 de la Couronne, Quebec, QC, G1K 9A9, Canada, alain.mailhot@ete.inrs.ca

*Corresponding author, tel.: 1-418-654-3776, fax: 1-418-654-2600

Word count: 10,172 (7,772+ 3 tables + 9 figures)

ABSTRACT

A new method to identify pipes with insufficient hydraulic capacity is proposed. This method can be applied to assess the future evolution of network performance under climate change (CC). It is based on hydrologic/hydraulic simulations using the Storm Water Management Model (SWMM) and single observed rainfall events. The evolution of the hydraulic performance with time is simulated by increasing the intensity of these rainfall events by a factor depending on the CC predictions for the study area. The proposed method is applied to two Canadian separated and combined sewer networks. The method identified the constraining pipe sections that could cause hydraulic dysfunctions in the networks, both in current and future climates. For the two networks, the number of constraining pipes depends on rain events and is anticipated to increase in the future climate. The proposed method can be applied to various types of networks to assess the network performance and project the evolution of the hydraulic performance of individual pipes over time, making it a useful tool for the planning of drainage network renewal under CC.

KEYWORDS

Constraining pipes; Renewal planning; Sewer network; SWMM model; Urban drainage

INTRODUCTION

The design of sewer pipes depends on their intended use (i.e., nature of the water to convey — wastewater, stormwater, or combined) and the peak flows they need to convey (Mailhot and Duchesne, 2010; Rosenberg *et al.*, 2010; Mailhot *et al.*, 2007b). More specifically, the diameters of stormwater and combined network pipes are determined to convey a critical flow corresponding to a rain event with a given return period, typically varying from two to five years. Increases in the imperviousness of the drained area and/or an increase in the intensity of the rain event corresponding to the design return period may reduce the hydraulic performance of sewer pipes (Li *et al.*, 2018; Kang *et al*., 2016; Neumann *et al.*, 2015; Berggren *et al.*, 2012; Jung *et al.*, 2011; Kleidorfer *et al.*, 2009; Olsson *et al.*, 2009; Mailhot *et al.*, 2008; Semadeni-Davies *et al.*, 2008; Niemczynowicz, 1982). In recent decades, climate change (CC) has led to an increase in the frequency of intense rainfall events in several regions of the world (see Miao *et al.*, 2019; Westra *et al*., 2015; IPCC, 2013; Ryu *et al*., 2014; Shephard *et al.*, 2014; Groisman *et al.*, 2005), and the available projections of extreme rainfall suggest that the intensity and frequency of extreme rainfall will continue to increase over the course of the twenty-first century (see Giorgi *et al.*, 2019; Dale *et al*., 2017; Kendon *et al.*, 2014; Westra *et al.*, 2014; IPCC, 2013; Mailhot *et al.*, 2012). According to several researchers, including Ruiter (2012), such changes may lead to more-frequent flooding and sewer backups. The development of hydraulic performance assessment tools for sewer networks, therefore, becomes crucial in the CC context. In this study, “hydraulic performance” refers to the possibility that a hydraulic dysfunction (surcharge, sewer backup, or flooding) will occur in a given network for a rainfall event corresponding to a given return period. Existing tools evaluating this performance and its evolution over time are based on two approaches — a statistical approach and hydraulic/hydrological (HH) modeling — or a combination of those two approaches (Babani *et al.*, 2008).

In the statistical approach, statistical models predict the deterioration of the hydraulic performance of individual sewer pipes over time as a function of factors related to the pipe characteristics (e.g., age and diameter) and the environment (e.g., soil type). Included among these models are: 1) fuzzy logic models, used by Hosseini and Ghasemi (2012) to estimate the Manning roughness coefficient to calculate the hydraulic performance values of individual pipes in a separate wastewater sewer; 2) ordered probit models and probabilistic neural-network models (Tran *et al.*, 2010), which express the probability that a pipe (stormwater network) will be in a given hydraulic performance state after a certain period of time depending on several factors (structural state condition, age of pipe, size, burial depth, slope, and soil type); and 3) Markov models, multiple discriminant analyses, and neural-network models (see Tran, 2007).

Despite their ability to predict the evolution in time of the hydraulic performance of individual sewer pipes, existing statistical models do not consider the climatic conditions or their changes over time, which are determinant factors in the pipes' hydraulic performance. Indeed, in the studies cited above, only the age of the pipes was modified to evaluate the future hydraulic performance of sewer pipes, and not the possible variation in time of climatic conditions. HH modeling can, however, address this issue.

An HH model can simulate the main processes involved in urban hydrology considering climatic conditions and urban development (Berggren *et al.*, 2012; Kleidorfer *et al.*, 2009; Olsson *et al.*, 2009; Niemczynowicz, 1989). In previous studies, future rain events representing future climatic conditions were constructed using different methods. The simplest method is to apply a relative increase to the intensity of a given design storm, the value of this increase being generally based on available climatic projections (Kirshen *et al*., 2015; Huong and Pathirana, 2013; Olsson *et al.*, 2013; Kleidorfer *et al.*, 2009; Watt *et al.*, 2003; Waters *et al.*, 2003; Niemczynowicz, 1989). A second method uses projections from climate models to modify observed rainfall series (Dale *et al.*, 2017; Berggren *et al.*, 2012; Olsson *et al.*, 2009; Semadeni-Davies *et al.*, 2008; Mailhot *et al.*, 2007b; He *et al.*, 2006). Another is based on the simulation of either future rainfall series or design storms derived by downscaling the output series from climate models (Kang *et al*., 2016; Osman, 2015). Finally, Dale *et al.* (2017) relied on the climate analog approach to estimate future changes in rainfall intensities.

Unlike studies using statistical models, most of those based on HH models assess the hydraulic performance of the whole sewer system, or of some part of it, but not the hydraulic performance of individual pipes (Berggren et al., 2012 and 2014; Dale et al., 2017; Denault et al., 2006; Huong and Pathirana, 2013; Kirshen et al., 2015; Kleidorfer et al., 2009; Mikovits et al., 2017; Niemczynowicz, 1989; Olsson et al., 2009; Semadeni-Davies et al., 2008; Waters et al., 2003; Watt et al., 2003; see the Supplementary Information for more details). Only a few studies have, to our knowledge, developed methodologies based on HH modeling capable of attributing a hydraulic performance condition to each pipe. This is the case for Bennis *et al.* (2003), who developed an index relating the hydraulic performance of a pipe to the height of maximum surcharge in the node located immediately upstream, for a given rainfall, and to the depth at which the pipe is buried. This performance index was also used in Tagherouit *et al.* (2011). In both of these studies, the CC impact was not considered.

To include the impact of CC, and in response to an increasingly urgent need for tools to assist in the planning of sewer renewal, a method is proposed in this study for the evaluation and prediction of the individual hydraulic performance of stormwater and combined sewer pipes in a changing climate. This method aims at identifying the pipes that should be upgraded to avoid hydraulic dysfunctions for specific rainfall events, in current and future conditions. It is based on: 1) the identification of the sections of pipe having a current unsatisfactory hydraulic performance, causing hydraulic dysfunctions (surcharge) in the network, and (2) the assessment of the evolution of the hydraulic capacity of pipes over time, as a function of the projected changes in rainfall intensities. The main originality of the proposed method is that it targets individual pipes that are responsible for current and future hydraulic dysfunctions in a CC context, pipes that could be replaced to maintain adequate long-term hydraulic performance. Such a strategy allows managers to prioritize and better plan pipe renewals.

The proposed method is based on HH modeling using the SWMM model (Rossman, 2008) with single observed rainfall events (SOREs), modified to represent future climatic conditions over several future horizons. Applications are presented for two real networks. Further details about the methodology are given in below.

METHODOLOGY

Case studies

The proposed method was applied to two sewer networks located in the province of Quebec (Canada), called A and B in the following for reasons of confidentiality. Network A corresponds to a mixed separated stormwater and combined sewer with a total pipe length of 46 km (0.125 to 1.8 m in diameter) that drain an area of 378 ha (23% impervious). Network B is a 70-km combined sewer network draining 475 ha (36% impervious), with pipe diameters varying from 0.15 to 3.8 m. The components of these two networks, as modeled in the SWMM, are illustrated in Figure 1. The calibrated SWMM models for these two areas were provided by their respective managers. Their calibration used the following information: 1) for Network A, five rainfall events (of recurrence up to five years), recorded by two rain gauges within the sector, and flow measurements collected between July and August 2011 (Fortier, V., Gagnon, J.F., Pugin, S., Trudel, L., Rapport final: Modélisation, calibration, diagnostic, solutions conceptuelles et études préparatoires (in french), Unpublished report); and 2) for Network B, two campaigns of flow measurements carried out over two distinct periods (from September 17 to October 16, 2014, and from August 25 to September 23, 2015) and observed rainfall data for these same periods (according to communications with the Municipality B).

Rain events

Modeling the hydraulic performance of pipes was carried out using observed SOREs, which were modified to take into account CC. Using such events allows: 1) more-realistic temporal distributions and intensities, as opposed to design storms; 2) targeting events that are likely to lead to sewer surcharge, backups, and flooding (Ruiter, 2012); and 3) reducing simulation time, which can become an issue when simulating continuous rainfall series (Notaro *et al.*, 2016).

From 5-min rainfall series recorded from 1943 to 1994 and from 1961 to 1976 at two meteorological stations located in southern Quebec, 400 events were extracted. Each rainfall event was characterized according to its return period for nine durations ranging from 5 min to 24 h. This characterization was based on the intensity–duration–frequency curves created by Mailhot and Talbot (2011) and by Villeneuve *et al.* (2007) using maximum annual precipitation series recorded at the same meteorological stations between 1943 and 1994. For the current analysis, only SOREs with return periods ranging from two to five years for at least one of the selected durations (5 min to 24 h), and without any return period higher than five years for these same durations, were selected. The 2 to 5 years return period criterion was retained, because it corresponds to the design criterion of pipes for the studied areas (consequently, surcharges should be avoided for the events corresponding to this design criterion). Only six of the 400 recorded events fulfilled this selection criterion. Figure 2 gives the rainfall profiles for these six SOREs, while Table 1 summarizes their characteristics. The selected SOREs show durations ranging from 1 to 24 h and variable temporal distributions. As shown in

Figure 2, their maximum intensity occurs either at the beginning, in the middle, or at the end of the event. To assess the impact of CC on the hydraulic performance of sewers, these SOREs were modified as described in the next section.

Climate change impact

According to Mailhot *et al.* (2007a), the intensity of extreme rainfall events of durations ranging from 1 to 24 h for less than 20-year return periods could increase by 15% in the future (2041-2070) compared to the current period (1961-1990) in southern Quebec. These results were obtained based on CRCM (Canadian Regional Climate Model) simulations for the SRES A2 scenario (Christensen *et al.*, 2007). More recently and for the same region, Mailhot *et al.* (2012) showed that the intensity of maximum annual precipitation for 6-, 12-, 24-, 72-, and 120-h durations and for 2-, 5-, 10-, and 20-year return periods (simulated by several regional climate models, driven by different global models and considering historic greenhouse gas concentrations for historical climate and the SRES A2 scenario for future periods) should increase by 10% to 20% between past (1968-2000) and future (2041-2070) periods.

Based on these conclusions, an increase of 15% in intensity over the next 25 years was chosen for the six selected SOREs. The rainfall intensity at each 5-min time step of the SOREs was multiplied by a factor to construct rainfall events representing the future climate. It was assumed that this factor varies linearly over the coming 25 years, so the future rainfall intensities were computed with:

$$I(t) = I_0 + (I_k - I_0)\frac{t - t_0}{t_k - t_0} \tag{1}$$

where $I(t)$ = rainfall intensity at year t, I_0 = rainfall intensity at year t_0 (reference period; original SORE), I_k = rainfall intensity at year t_k ($I_k = 1.15\ I_0$ in our case), and t_k = year of climate forecasts ($t_k - t_0 = 25$ years in our case).

The hypothesis of linearity of the evolution of rain intensities over time for the same return period has been already adopted by Mailhot and Duchesne (2010). Moreover, the linearity hypothesis can be justified because the planning horizon is relatively short compared with the time scale over which the signal of CC will emerge.

Proposed method to assess the current and future hydraulic performance of sewer pipes

As mentioned, hydraulic performance refers to the pipes' capacity to fulfill their role of draining stormwater from an event with a given return period without any backup or flooding. Pipe surcharge generally has an impact on upstream flow, raising the hydraulic grade line. Beyond a critical level, the rise of the hydraulic grade line can cause backups in basements and, eventually, flooding at the surface.

The proposed method identifies the constraining pipes that are responsible for hydraulic dysfunction (HDsf) in the network, for a specific rain event, through three main steps.

- *Step 1: Localization of all HDsf in the network, based on the SWMM hydraulic simulation results.* As shown in Figure 3, an HDsf occurs when the water height at a node exceeds the crown level of the neighboring downstream pipe.
- *Step 2: Delimitation of a perimeter of influence (PI) for each detected dysfunction.* A *PI* is defined as the set of adjacent surcharged pipes. Each *PI* stops at the first upstream and downstream nodes that are not surcharged, as shown in Figure 3.

- Step 3 (Figure 4): Identification of the pipe(s) that are responsible for the hydraulic dysfunctions in each *PI*.
    i. A reference node (*RN*) is first identified (Figure 4, Block 1) as well as the pipes that could be responsible for the HDsf in the studied *PI* (referred here as “potentially constraining pipes,” **PCPs**). As shown in Figure 3, *RN* corresponds to the node with the highest water level in the *PI*. **PCPs** are necessarily located downstream of the *RN* (as shown in Figure 3, **PCP** = {P_1; P_2; ….; P_n}, ordered from upstream to downstream, where P_n is the pipe located at the downstream end of *PI,* and P_1 is the pipe immediately downstream of *RN*). In the proposed method, a matrix containing all possible combinations of potentially constraining pipes (**M_PCP**) is first constructed (Figure 4, Block 1). The number of rows (n) in **M_PCP** equals the number of pipes in **PCP**.

$$\boldsymbol{M\_PCP} = \begin{bmatrix} P_1 & . & . & P_{n-2} & P_{n-1} & P_n \\ . & . & . & . & & \\ P_{n-2} & P_{n-1} & P_n & & & \\ P_{n-1} & P_n & & & & \\ P_n & & & & & \end{bmatrix}$$

ii. Starting with **PCP**, the pipes that are responsible for the HDsf in *PI* (the constraining pipes) are identified (Figure 4, Block 2). This is done in a loop, for which, during each iteration, the pipes that are analyzed to determine whether they are constraining are called the evaluated pipes, **EP**. As shown in Figure 4, for the first iteration, **EP** = $\{P_n\}$ (the most downstream pipe in *PI*), i.e., the last row in **M_PCP**, and then, if required, the identification of the constraining pipes is performed for each row of **M_PCP** in decreasing order. To estimate whether the **EP** are constraining, all their respective hydraulic capacities (diameters) are progressively increased until the dysfunction disappears or until the diameter of the smallest pipe immediately downstream of P_n (P_{n+1}) is reached. When the dysfunction disappears after increasing the diameter of the pipe(s) in **EP**, without reaching the diameter of the pipe downstream of P_n, these pipes are identified as constraining, i.e., responsible for the HDsf (Figure 4, Block 2-a). In the opposite case (Figure 4, Block 2-b), i.e., if the diameter of the pipe downstream of P_n is reached and a surcharge still subsists, pipes in **EP** are considered not to be the sole constraining pipes for the HDsf, and the pipes in the preceding row in **M_PCP** (**EP** = **M_PCP**$_{\mathbf{n-1}}$) are considered. This process is repeated until the dysfunction disappears or until the first row of **M_PCP** is reached (**EP** = **M_PCP**$_{\mathbf{1}}$ = $\{P_1; \ldots; P_{n-1}; P_n\}$). When the HDsf persists despite increasing the diameter of all pipes in **M_PCP**$_{\mathbf{1}}$ (Figure 4, Block 2-c), **PCP** is expanded to contain P_{n+1}, the pipe downstream of P_n, which becomes the last pipe of the new **PCP** (new

P_n). If one or more pipes downstream of the new P_n have the same diameter as this new P_n, these pipes ($\mathbf{P_{DW}}$ in Figure 4: vector of a whole series of pipes downstream of the new P_n having the same diameter as P_n) are included in the new **PCP**, and the most downstream pipe of $\mathbf{P_{DW}}$ becomes the new P_n. The identification of constraining pipes is then carried out using the new **PCP**. In the case P_{n+1} is an outlet or storage pipe, no pipe is identified as constraining for the HDsf in the *PI* (Figure 4, Block 2-d).

The projected change in hydraulic performance caused by CC was simulated for each selected SORE (Table 1 and Figure 2) at regular intervals of five years, as shown in Figure 5. Five-year intervals were chosen, as that interval is characteristic of the period generally considered by networks managers for carrying out priority interventions (see MAMROT, 2013).

At each time step, Equation 1 is used to modify the rain intensities to obtain events corresponding to each of the six time horizons, from the first or current horizon (H_1) to the last one (H_6), 25 years later, and the constraining pipes are identified for each of these horizons.

RESULTS AND DISCUSSION

Using the selected SORE, the proportions of surcharged nodes (SNs) and those that are at risk of flooding (NRFs, i.e., for which the maximum water level is less than 1 m below the ground level) in Networks A and B in their current state (i.e., without any modification in their pipes' diameters) are given in Table 2 for the first and last horizons. Table 2 shows that increasing rainfall intensities over the time horizons, from H_1 to H_6, leads to increases in the proportion of SNs and NRFs. According to the results in Table 2, the proportions of nodes that are currently (H_1) surcharged or at risk of flooding vary slightly (from 1% to 7%) from one event to the other for Network A but strongly depend on the event for Network B. These differences could be caused by the varying density of nodes in different parts of the networks (e.g., many nodes in areas that become surcharged for some events but are not for the others). For Networks A and B, a Spearman rank correlation test (Sheskin 2003) showed no relationship between these three SORE characteristics — i) duration, ii) maximal intensity over 5 min (I_{max_5min}), and iii) total height — and the proportions of SN, NRF, and total length of constraining pipes (TLCP) for the six events. The same result is obtained for the six horizons, except for the fifth one, where a possible dependency is obtained between event duration and the proportion of TLCP.

When applied to Networks A and B, the proposed method (see Figure 4) identified the constraining pipes that are responsible of each surcharge, either in current or in future conditions. These pipes have an insufficient hydraulic capacity, and the presented method proposes the required pipe diameters to ensure free surface flow in the entire network for the selected six SOREs (recurrence less than five years). Table 2 gives the proportion of constraining pipes for the six events for the first and last horizons, while Figure S-1, in the Supplementary Information, shows its evolution over the six horizons.

Figure 6 shows how constraining pipes are identified for some HDsf in Network A, for the first horizon (H_1), and for Event 1. In this example, as for the other events and horizons, the SNs are first grouped by *PI*, represented by green polygons in Figure 6. Then the constraining pipes for each *PI* are identified (red pipes in Figure 6). The constraining pipes can be identified either: i) during the first iteration of the method (see Figure 4) (in this case the constraining pipes are in the vicinity of the SN) or ii) after the increase of the diameters of some other pipes located downstream of the SN. Therefore, no surcharge is illustrated in Figure 6 close to some of the constraining pipes.

As illustrated in Figure 6, one single pipe can be responsible (constraining) for a surcharge area including several nodes and pipes, such as in Case 1. Case 2 (Figure 6) gives an example of pipes that were considered constraining, even if they were not located in the surcharge zone (*PI*), because their diameter is the same as the diameter of the most downstream pipe in the *PI*, and, thus, their diameter needs to be increased to eliminate the HDsf in this *PI*. Figure 6 also shows an example of an HDsf located upstream of an outlet or storage (Case 3), which is considered a special case where the surcharge is allowed and does not require any modification in the network.

Table 3 gives an example of some of the constraining pipes, their current diameter, and the proposed diameter to eliminate the HDsf, for the six considered horizons of the most problematic events (MPEs, which cause the largest number of surcharges) for Networks A and B, namely, Events 2 and 3, respectively. Network A is characterized by smaller and more impermeable subcatchments than Network B. This may explain why: 1) Network A is more sensitive to Event 2, which has the highest maximal intensity over 5 min and occurs over a shorter duration (in this case, runoff is quicker and more important), and 2) surcharges in Network B are more important for Event 3, which generates the largest volume and lasts longer (in this case, surcharges are more sensitive to soil saturation).

In Network A in its current form (no pipes replaced), from 10% to 12% of the total length of pipes was identified as constraining, or responsible, for the HDsf (and, thus, would eventually need to be replaced by larger pipes) between H_1 and H_6 of the MPE (Event 2, see Figure S-1a). For Network B, 14% to 23% of the total length of pipes (with diameter between 150 mm and 3.5 m) has an insufficient hydraulic capacity (Event 3, Figure S-1b). The samples of pipes presented in Table 3 cover a wide range of diameters and give only some examples of pipes that become constraining with time. Some pipes have an insufficient current (H_1) hydraulic capacity, such as pipes UNI_154697 and 70820 of Network A and B, respectively, while others will be constraining only at the sixth horizon, such as the pipes PLU_1062127 (Network A) and 108287 (Network B). In some cases, one or more pipes can be identified as being constraining at a given horizon and not at following time horizons (e.g., pipe DOM_153912 of Network A and 70821 of Network B). Moreover, some of the identified constraining pipes require less hydraulic capacity at future horizons than at earlier ones (e.g., pipe 70820 in Network B). These last two situations can be explained by the fact that constraining pipes located downstream of the initial ones may be identified when rainfall intensity is increased at future time horizons. These increases can result in surcharges farther downstream of initially considered constraining pipes. Increasing the hydraulic capacity of downstream pipes therefore eliminates the surcharges in the most upstream pipes.

In both networks, the diameter of constraining pipes can be slightly or greatly upgraded, depending on rainfall events. The upgraded diameter can, in some cases, be more than four times the current one, as for pipe PLU_296060 in Network A, or slightly larger, as for pipe UNI_157023 in Network A. Moreover, the proposed diameters might not change, in some cases, over the six horizons (from H_1 to H_6); on the contrary, they may increase with the increase in rainfall intensity for some horizons (e.g., pipe 70947 in Network B).

Table 2 and Figure S-1 shows the evolution of the proportion of constraining pipes over the six horizons and for the six events. According to these results, the first three events (1, 2, and 3) are those that cause the largest number of surcharges, either in Network A or Network B. The first two events are characterized by the highest I_{max_5min}, and the largest part of their total height occurs over a short period (from 1.0 h to 1.5 h, see Figure 2). As for Event 3, it has the highest total height.

Likewise, for both networks, there is an obvious increase in the proportions of SN and NRF, and, consequently, in proportions of TLCP, with increasing rainfall intensity, i.e., from H_1 to H_6. In the case of Network A, these proportions, as well as their evolution in time, are slightly different from one SORE to the other. Regarding the proportion of

TLCP, despite the largest increase for the last three SOREs, one can see higher proportions for the first three events in Network A. For this network, the proportion of TLCP increases by 25% (reaching 12%) for the MPE between H_1 and H_6. In the case of Network B, still for the MPE, this proportion of TLCP increases by 61% from H_1 to H_6. Constraining pipes represent 23% of the total length of pipes at the sixth horizon in Network B, which is almost double that of Network A. This is because Network B is highly surcharged, even in the current climate (H_1). Thus, even a small increase in rainfall intensity leads to a sharp increase in the proportions of SN and TLCP. The recorded variability in the proportions of SN, NRF, and TLCP as a function of SORE could be explained by the variability in these event distributions.

Figures S-2 and S-3, in the Supplementary Information, give the localization of constraining pipes in Networks A and B for the first and sixth horizons using the MPE for each network.

Given the variability of results between each SORE, constraining pipes obtained with the MPE (Event 2 for Network A and Event 3 for Network B) were first considered to identify the pipes to be replaced in Networks A and B. Afterward, it was verified whether the replacement of these pipes led to the elimination of all surcharge problems with the five other events and for all six time horizons. For Network A, three additional constraining pipes had to be added to those determined with the MPE, whereas, for Network B, the replacement of the constraining pipes determined with the MPE was sufficient to eliminate all surcharges with the six SOREs and the six time horizons.

CONCLUSION

In this research, a novel method was proposed to assess and predict the hydraulic performance of individual sewer pipes in current and future climates. This method is based on hydraulic and hydrologic modeling with single observed extreme events, representing a specified design recurrence (from two to five years in this case) and a wide range of durations, time distributions, and intensities. The proposed method consists of locating hydraulic dysfunctions, isolating them, and identifying the pipe or pipes that are constraining for these dysfunctions. The identification of the constraining pipes was carried out by increasing their hydraulic capacity until the dysfunction disappeared. The evolution in time of the sewer pipes' hydraulic performance was simulated by increasing the intensity of the rainfall events used as inputs for the simulations. This method was applied to two different areas of Canadian sewer systems. In both cases, the proposed method made it possible to: 1) identify the constraining pipe(s) for the hydraulic dysfunctions caused by rain events representing each evaluated horizon and 2) propose the required diameters to maintain an acceptable level of service for the studied networks. This application showed that Networks A and B reacted differently to the same events. More surcharges and pipes to be replaced were identified for Network B, even for less intense events. This network is also the one that is the most sensitive to CC, because it is already highly surcharged in current climate. Moreover, Network B is more sensitive to events having larger total heights, while Network A is more sensitive to events with the higher maximal intensities over 5 min. These variations of results for the two studied networks and between rain events show the importance of considering various rainfall events for the design and analysis of drainage networks, either in the current climate or in a CC context.

The presented method is automated and can be easily applied to other and different types of network using any desired input rainfall to predict the individual pipes' hydraulic performance over time, making it a useful tool for the planning of drainage network renewal. It should be noted however that the replacement of pipes is not the only option available to adapt sewer systems to the increase of runoff in urban areas. Source control measures should also be taken into account when attempting to prevent backflows, overflows, and sewer backups. In future work, the method presented here will be integrated in a methodology aiming at scheduling adaptation measures over time, including pipe replacement and installation of source control measures, taking into account economic factors and climate change. Ideally, the structural and hydraulic deterioration processes should be taken into account simultaneously in this methodology. It could then be verified how the integration of different adaptation measures (installation of source control, replacement of pipes, retrofitting, etc.) makes it possible to reduce the total costs of renewal interventions while improving the overall performance of sewer networks.

DATA AVAILABILITY STATEMENT

The rainfall data, the characteristics of sewers and the SWMM models used during the study were provided by third parties. Direct requests for these materials may be made to the providers; the corresponding author can provide the contact information of these providers on request. The codes generated during the study are available from the corresponding author by request.

ACKNOWLEDGEMENTS

The authors wish to thank the two anonymous municipalities for providing the SWMM networks SWMM model used in this study. The authors are also grateful to Guillaume Talbot for his help in programming.

.

NOTATION LIST

CC	Climate Change
DC	Delta Change
DFC	Delta Change Factor
EP	Evaluated Pipes
GHG	Greenhouse Gas
HDsf	Hydraulic Dysfunction
HH	Hydraulic/Hydrological
Imax_5min	Maximal Intensity over 5 Min
MPE	Most Problematic Event
NRF	Node at Risk of Flooding
P_1	Upstream-Most Pipe in the Ensemble of Potentially Constraining Pipes
P_{DW}	Vector of Pipes Downstream of P_n Having the Same Diameter as P_n
P_n	Downstream-Most Pipe in the Ensemble of Potentially Constraining Pipes
PCP	Potentially Constraining Pipe
PI	Perimeter of Influence
RN	Reference Node
SN	Surcharged Node
SORE	Single Observed Rainfall Event
TLCP	Total Length of Constraining Pipes

REFERENCES

Babani, J., Adams, B.J., and Wilson, B.G. (2008). “Integrating hydraulic and environmental performance assessments in asset management of wastewater collection networks.” *Proc., 11th International Conference* on Urban Drainage, Edinburgh, Scotland, UK.

Bennis, S., Bengassem, J., and Lamarre, P. (2003). “Hydraulic performance index of a sewer network”. *Journal of Hydraulic Engineering,* doi: 10.1061/(ASCE)0733-9429(2003), 129(7), 504-510.

Berggren, K., Olofsson, M., Viklander, M., Svensson, G., and Gustafsson, A.M. (2012). “Hydraulic impacts on urban drainage systems due to changes in rainfall caused by climatic change.” *J. Hydrol. Eng.*, doi: 10.1061/(ASCE)HE.1943-5584.0000406,17(1), 92-98.

Berggren, K., Packman, J., Ashley, R., and Viklander, M. (2014). “Climate changed rainfalls for urban drainage capacity assessment.” *Urban Water J.,* doi: 10.1080/1573062X.2013.851709, *11*(7), 543-556.

Christensen, J.H., Hewitson, B., Busuioc, A., Chen, X., Gao, X., Held, I., Jones, R., Kolli, R.K., Kwon, W.-T., Laprise, R., Magaña Rueda, V.M., Mearns, L., Menéndez, C.G., Räisänen, J., Rinke, A., Sarr, A. and Whetton, P. (2007). “Regional Climate Projections.” *In: Climate Change 2007: The Physical Science Basis. Contribution of Working Group I to the Fourth Assessment Report of the Intergovernmental Panel on Climate Change [Solomon, S., D. Qin, M. Manning, Z. Chen, M. Marquis, K.B. Averyt, M. Tignor and H.L. Miller (eds.)]. Cambridge University Press, Cambridge, United Kingdom and New York, NY, USA.*

Dale, M., Luck. B., Fowler, H.J., Blenkinsop, S., Gill, E., Bennett, J., Kendon, E. and Chan, S. (2017). “New climate change rainfall estimates for sustainable drainage.” Proc. Inst. Civ. Eng.: Engineering Sustainability, doi:10.1680/jensu.15.00030, 170(ES4), 214-224, in press

Denault, C., Millar, R.G., and Lence, B.J. (2006). “Assessment of possible impacts of climate change in an urban catchment.” *J. Am. Water Resour. Assoc.*, doi: 10.1111/j.1752-1688.2006.tb04485.x, 42(3), 685-697.

DHI [Computer software], (2013). “MIKE URBAN - Modeling Water in the City.” {http://mikebydhi.com/Products/Cities/MIKEURBAN.aspx} (June 15 2017)

Gibbons, R.D., and Coleman, D.E. (2001). Statistical methods for detection and quantification of environmental contamination. *John Wiley and Sons, Wiley, New York.*

Giorgi, F., Raffaele, F., and Coppola, E. (2019). “The response of precipitation characteristics to global warming from climate projections.” Earth Syst. Dynam., doi: 10.5194/esd-10-73-2019, 10(1), 73-89.

Groisman, P.Y., Knight, R.W., Easterling, D.R., Karl, T.R., Hegerl, G.C., and Razuvaev, V.N. (2005). “Trends in intense precipitation in the climate record.” *J. Clim.*, doi: 10.1175/JCLI3339.1, 18(9), 1326-1350.

He, J., Valeo, C., and Bouchart, F.C. (2006). “Enhancing urban infrastructure investment planning practices for a changing climate.” Water Sci. Technol., doi: 10.2166/wst.2006.292, 53(10), 13-20.

Hosseini, S.M., and Ghasemi, A. (2012). “Hydraulic performance analysis of sewer systems with uncertain parameters.” *J. Hydroinf.*, doi: 10.2166/hydro.2011.129, 14(3), 682-696.

Huong, H.T.L., and Pathirana, A. (2013). “Urbanization and climate change impacts on future urban flooding in Can Tho City, Vietnam.” *Hydrol. Earth Syst. Sci.*, doi: 10.5194/hess-17-379-2013, 17: 379-394.

Innovyze (2018). “Innovyze InfoWorks CS (Collection Systems) – Overview.” {http://www.innovyze.com/products/infoworks_cs/} (March 19 2018).

IPCC (2013). “Climate Change 2013: The Physical Science Basis.” *Contribution of Working Group I to the Fifth Assessment Report of the Intergovernmental Panel on Climate Change* [Stocker, T.F., D. Qin, G.-K. Plattner, M. Tignor, S.K. Allen, J. Boschung, A. Nauels, Y. Xia, V. Bex and P.M. Midgley (eds.)]. Cambridge University Press, Cambridge, United Kingdom and New York, NY, 1535 pp.

Jung, I.W., Chang, H., and Moradkhani, H. (2011). “Quantifying uncertainty in urban flooding analysis considering hydro-climatic projection and urban development effects.” *Hydrol. Earth Syst. Sci.*, doi: 10.5194/hess-15-617-2011, 15(2), 617-633.

Kang, N., Kim, S., Kim, Y., Noh, H., Hong, S.J., and Kim, H.S. (2016). “Urban drainage system improvement for climate change adaptation.” *Water*, doi: 10.3390/w8070268 , 8(268), w8070268.

Kendon, E.J., Roberts, N.G., Fowler, H.J. Roberts, M.J. Chan, S.C., and Senior, C.A. (2014). “Heavier summer downpours with climate change revealed by weather forecast resolution model.” *Nat. Clim. Change*, doi: 10.1038/nclimate2258, 4, 570-576.

Kirshen, P., Caputo, L., Vogel, R.M., Mathisen, P., Rosner, A., and Renaud, T. (2015). “Adapting urban infrastructure to climate change: a drainage case study.” *J. Water Resour. Plann. Manage.*, doi: 10.1061/(asce)wr.1943-5452.0000443, 141(4).

Kleidorfer, M., Möderl, M., Sitzenfrei, R., Urich, C., and Rauch, W. (2009). “A case independent approach on the impact of climate change effects on combined sewer system performance.” *Water Sci. Technol.*, doi: 10.2166/wst.2009.520, 60(6), 1555-1564.

Li, C.L., Liu, M., Hu, Y.M., Shi, T., Qu, X.Q., and Walter, M.T. (2018). “Effects of urbanization on direct runoff characteristics in urban functional zones.” *Sci. Tot. Environ.*, doi: 10.1016/j.scitotenv.2018.06.211, 643, 301-311.

Lovino, M.A., Muller, O.V., Berbery, E.H., and Muller, G.V. (2018). “How have daily climate extremes changed in the recent past over northeastern Argentina*?” Global Planet. Change,* doi: 10.1016/j.gloplacha.2018.06.008, 168, 78-97.

Madsen, H., Arnbjerg-Nielsen, K., and Mikkelsen, P.S. (2009). “Update of regional intensity–duration–frequency curves in Denmark: tendency towards increased storm intensities.” *Atmos. Res.*, doi: 10.1016/j.atmosres.2009.01.013, 92(3), 343-349.

Mailhot, A., Beauregard, I., Talbot, G., Caya, D., and Biner, S. (2012). “Future changes in intense precipitation over Canada asses*sed from multi-model NARCCAP ensemble simulations.” Int. J. Climatol.*, doi: 10.1002/joc.2343, 32(8), 1151-1163.

Mailhot, A., and Duchesne, S. (2010). “Design criteria of urban drainage infrastructures under climate change.” *J. Water Resour. Plann. Manage.*, doi: 10.1061/ASCEWR.1943-5452.0000023, 136(2), 201-208.

Mailhot, A., Duchesne, S., Caya, D., and Talbot, G. (2007a). “Assessment of future change in intensity–duration–frequency (IDF) curves for Southern Quebec using the Canadian Regional Climate Model (CRCM).” *J. Hydrol.*, doi: 10.1016/j.jhydrol.2007.09.019, 347(1), 197-210.

Mailhot, A., Duchesne, S., Larrivée, C., Pelletier, G., Bolduc, S., Rondeau, F., Kingumbi, A., and Talbot, G. (2008). “Conception et planification des interventions de renouvellement des infrastructures de drainage urbain dans un contexte d'adaptation aux changements climatiques.” Research Report No. R920, *Institut National de la Recherche Scientifique INRS-Eau, Terre et Environnement, Quebec*, Canada, 170 p. (in French)

Mailhot A., Duchesne S., and Villeneuve J.-P. (2007b). ”Les changements climatiques : enjeux et perspectives en matière d’infrastructures urbaines.”. *Contact Plus*, 62: 20-26. (in French)

Mailhot, A., and Talbot, G. (2011). “Mise à jour des estimateurs Intensité-Durée-Fréquence (IDF) et Hauteur-Durée-Fréquence (HDF) pour le sud-Québec, Tome II-Résultats.”. *Research Report No R-1259, Institut National de la Recherche Scientifique INRS-Eau, Terre et Environnement, Quebec, Canada 285 p. (in French)*

MAMROT (2013). “Guide d’élaboration d’un plan d’intervention pour le renouvellement des conduites d’eau potable, d’égouts et des chaussées.“ *Centre d’expertise et de recherche en infrastructures urbaines et Ministère des Affaires municipales, des Régions et de l'Occupation du territoire du Québec, Montreal, Canada*, 87 p. (in French)

Miao, C.Y., Duan, Q.Y., Sun, Q.H., Lei, X.H., and Li, H. (2019). “Non-uniform changes in different categories of precipitation intensity across China and the associated large-scale circulations.” *Environ. Res. Lett.*, doi: 10.1088/1748-9326/aaf306, 14(2), 025004.

Mikovits, C., Tscheikner-Gratl, F., Jasper-Tönnies, A., Einfalt, T., Huttenlau, M., Schöpf, M., Kinzel, H., Rauch, W., and Kleidorfer, M. (2017). “Decision support for adaptation planning of urban drainage systems.” *J. Water Resour. Plann. Manage.*, doi: 10.1061/(ASCE)WR.1943-5452.0000840, 143(12), 04017069.

Min, S.K., Zhang, X., Zwiers, F.W., and Hegerl, G.C. (2011). “Human contribution to more-intense precipitation extremes.” *Nature*, doi: 10.1038/nature09763, 470(7334), 378-381.

Murphy, J.M., Sexton, D.M.H., Jenkins, G.J., Boorman, P., Booth, B., Brown, K., Clark, R., Collins, M., Harris, G. and Kendon, L. (2009). “*UK Climate Projections Science Report: Climate Change Projections*.” Met Office, Hadley Centre, Exeter, UK.

Neumann, J. E., Price, J., Chinowsky, P., Wright, L., Ludwig, L., Streeter, R., Jones, R., Smith, J. B., Perkins, W., Jantarasami, L., and Martinich, J. (2015). “Climate change risks to US infrastructure: impacts on roads, bridges, coastal development, and urban drainage.” *Clim. Change*, doi: 10.1007/s10584-013-1037-4, 131(1), 97-109.

Niemczynowicz, J. (1982). “Areal intensity-duration-frequency curves for short term rainfall events in Lund.” *Hydrol. Res.*, 13(4), 193-204.

Niemczynowicz, J. (1989). “Impact of the greenhouse effect on sewerage systems—Lund case study.” *Hydrol. Sci. J.*, doi: 10.1080/02626668909491373, 34(6), 651-666.

Notaro, V., Fontanazza, C.M., La Loggia, G., and Freni, G. (2016). “Flood frequency analysis for an urban watershed: comparison between several statistical methodologies simulating synthetic rainfall events.” *J. Flood Risk Manage.*, doi: 10.1111/ jfr3.12283, 26, 3904-3918.

Olsson, J., Amaguchi, H., Alsterhag, E., Dåverhög, M., Adrian, P.E., and Kawamura, A. (2013). “Adaptation to climate change impacts on urban storm water: A case study in Arvika, Sweden.” *Clim. Change*, doi: 10.1007/s10584-012-0480-y, 116(2), 231-247.

Olsson, J., Berggren, K., Olofsson, M., and Viklander, M. (2009). “Applying climate model precipitation scenarios for urban hydrological assessment: A case study in Kalmar City, Sweden.” *Atmos. Res.*, doi: 10.1016/j.atmosres.2009.01.015, 92(3), 364-375.

Osman, Y.Z. (2015). “Monitoring the future behaviour of urban drainage system under climate change: a case study from north-western England.” *Open Engineering*, doi: 10.1515/eng-2015-0003, *5(1)*, 1-5.

Powell, A. (2008). “An analysis of the change of design storms due to future climate predictions.” M.S. thesis, University of Colorado, Boulder, CO, 95 p.

Rosenberg, E.A., Keys, P.W., Booth, D.B., Hartley, D., Burkey, J., Steinemann, A.C., and Lettenmaier, D.P. (2010). “Precipitation extremes and the impacts of climate change on stormwater infrastructure in Washington State.” *Clim. Change*, doi: 10.1007/s10584-010-9847-0, *102*(1), 319-349.

Rossman, L.A. (2008). Storm Water Management Model User's Manual, version 5.0. *National Risk Management Research Laboratory, Office of Research and Development, US Environmental Protection Agency*, Cincinnati, OH, USA.

Ruiter, A. (2012). “Delta-change approach for CMIP5 GCMs.” *Trainee Report, Royal Netherlands Meteorological Institute*.

Ryu, J., Lee, H., Yu. S., and Park. K. (2014). “Statistical evaluation on storm sewer design criteria under climate change in Seoul, South Korea.” *Urban Water J.*, doi: 10.1080/1573062X.213.801498, 11(5), 370-378.

Semadeni-Davies, A., Hernebring, C., Svensson, G., and Gustafsson, L.G. (2008). “The impacts of climate change and urbanisation on drainage in Helsingborg, Sweden: Combined sewer system.” *J. Hydrol.*, doi:10.1016/j.jhydrol.2007.05.028, 350(1), 100-113.

Shephard, M.W., Mekis, E., Morris, R.J., Feng, Y., Zhang, X., Kilcup, K., and Fleetwood, R. (2014). “Trends in Canadian short-duration extreme rainfall: Including an intensity-duration-frequency perspective.” *Atmos. Ocean*, doi: 10.1080/07055900.2014.969677, 52(5), 398-417.

Sheskin, D.J. 2003. Handbook of Parametric and Nonparametric Statistical Procedures. 3rd ed. *Chapman and Hall/CRC*, New York, NY.

Tagherouit, W.B., Bennis, S., and Bengassem, J. (2011). “A fuzzy expert system for prioritizing rehabilitation of sewer networks.” *Computer-Aided Civil and Infrastructure Engineering*, doi: 10.1111/j.1467-8667.2010.00673.x, 26(2), 146-152.

Tran, D.H., (2007). "Investigation of Deterioration Models for Stormwater Pipe Systems." Ph.D. thesis. *School of Architectural, Civil and Mechanical Engineering, Victoria University, Melbourne, Australia,* 219 p.

Tran, D.H., Perera, B.J.C., and Ng, A.W.M. (2010). "Hydraulic deterioration models for storm-water drainage pipes: ordered probit versus probabilistic neural network." *J. Comput. Civil Eng.*, doi: 10.1061/(ASCE)CP.1943-5487.0000020, 24(2), 140-150.

Villeneuve, J.-P., Duchesne, S., and Mailhot, A. (2007). "Analyse de la pluviométrie récente sur le territoire de la ville de Québec et pronostics d'évolution dans un contexte de changements climatiques. " Research Report R-911f, Institut National de la Recherche Scientifique INRS-Eau, Terre et Environnement, Quebec, Canada, 156 p. (in French)

Waters, D., Watt, W.E., Marsalek, J., and Anderson, B.C. (2003). "Adaptation of a storm drainage system to accommodate increased rainfall resulting from climate change." *J. Environ. Plann. Manage.*, doi: 10.1080/0964056032000138472, 46(5), 755-770.

Watt, W.E., Waters, D., and McLean, R. (2003). "Climate Change and Urban Stormwater Infrastructure in Canada: Context and Case Studies." *Toronto-Niagara Region Study Report and Working Paper Series Rep. No. 2003-1, Meteorological Service of Canada, Waterloo, Canada*.

Westra, S., Alexander, L. V., and Zwiers, F. W. (2015). "Global increasing trends in annual maximum daily precipitation." *J. Clim.*, doi: 10.1175/JCLI-D-12-00502.1, 26(11), 3904-3918.

Westra, S., Fowler, H.J., Evans, J.P., Alexander, L.V., Berg, P., Johnson, F., Kendon, E.J., Lenderink, G., and Roberts, N.M. (2014). “Future changes to the intensity and frequency of short-duration extreme rainfall.” *Rev. Geophys.*, doi: 10.1002/2014RG000464, 52, 522-555.

Zhou, Q., Mikkelsen, P.S., Halsnæs, K., and Arnbjerg-Nielsen, K. (2012). “Framework for economic pluvial flood risk assessment considering climate change effects and adaptation benefits.” *J. Hydrol.*, doi: 10.1016/j.jhydrol.2011.11.031, 414, 539-549.

Table 1. Characteristics of the selected six rainfall events, with return periods of two to five years for durations ranging from 5 min to 24 h

Events	Event characteristics			Recurrence per duration (years)								
	Total height (mm)	Maximum intensity over 5 min (mm/h)	Total duration (h)	5 min	10 min	15 min	30 min	1 h	2 h	6 h	12 h	24 h
1	20.1	91.5	0.92	2 to 5	2 to 5	2 to 5	2 to 5	< 2	< 2	< 2	< 2	< 2
2	28.9	103.7	1.67	2 to 5	2 to 5	2 to 5	2 to 5	2 to 5	< 2	< 2	< 2	< 2
3	53.0	54.9	9.17	< 2	< 2	< 2	2 to 5	2 to 5	2 to 5	2 to 5	< 2	< 2
4	29.4	61.0	2.08	< 2	< 2	< 2	2 to 5	2 to 5	2 to 5	< 2	< 2	< 2
5	42.0	62.7	24.00	< 2	< 2	< 2	2 to 5	2 to 5	2 to 5	2 to 5	< 2	< 2
6	48.7	47.6	23.42	< 2	< 2	< 2	< 2	2 to 5	2 to 5	2 to 5	2 to 5	< 2

Table 2. Proportion of surcharged nodes, of nodes at risk of flooding and of total length constraining pipes in Networks A and B for the six selected rainfall events and the short-term (H1) and long-term (H6) horizons

Events	Network A						Network B					
	Proportion of surcharged nodes - SN (%)		Proportion of nodes at risk of flooding - NRF (%)		Proportion of total length constraining pipes - TLCP (%)		Proportion of surcharged nodes - SN (%)		Proportion of nodes at risk of flooding nodes - NRF (%)		Proportion of total length constraining pipes - TLCP (%)	
	H_1	H_6	H_1	H_6	H_1	H_6	H_1	H_6	H_1	H_6	H_1	H_6
1	6	8	3	4	6	9	11	20	3	7	13	19
2	7	9	3	5	8	11	20	43	7	24	19	30
3	5	10	2	7	6	9	57	85	28	71	25	38
4	4	6	2	4	4	7	10	18	2	4	13	17
5	3	5	1	2	3	6	7	16	2	3	11	16
6	2	3	1	1	2	4	9	34	2	11	12	21

Table 3. Partial list of constraining pipes with their current and upgraded diameters for the six horizons for Network A (Event 2) and for Network B (Event 3) (~ means that the current diameter is adequate)

Network	Event	Pipe name	Current diameter (m)	Proposed diameter (m)					
				H_1	H_2	H_3	H_4	H_5	H_6
A	2	PLU_1062127	0.900	~	~	~	~	~	1.000
		UNI_154189	0.300	~	~	~	0.375	0.375	0.375
		UNI_157023	0.200	~	~	0.250	0.250	0.250	0.250
		PLU_33940a	0.375	~	0.625	0.625	0.625	0.625	0.625
		UNI_154697	0.450	0.600	0.600	0.750	0.600	0.600	0.600
		PLU_296060	0.200	0.950	0.950	0.950	0.950	0.950	~
		DOM_153912	0.600	~	~	0.750	~	~	~
		DOM_157235	0.250	0.375	~	~	0.375	0.375	~
B	3	108287	1.350	~	~	~	~	~	1.600
		70737	0.525	~	~	~	~	1.150	1.150
		70744	0.600	~	~	~	2.050	1.150	1.150
		73138	1.200	~	~	1.600	1.450	1.450	1.450
		71362	2.850	~	3.350	3.350	3.100	3.350	3.350
		70821	0.375	~	0.700	~	0.700	~	0.625
		70820	0.300	0.375	0.700	0.375	0.700	0.375	0.625
		70947	0.450	0.950	0.950	0.950	1.200	1.450	1.450

FIGURE CAPTIONS

Fig. 1. SWMM hydraulic models of Networks B (left) and A (right)

Fig. 2. Rainfall series (5-min time step) of the six rainfall events used in the analyses

Fig. 3. PI of hydraulic dysfunctions

Fig. 4. Method for identifying the pipes responsible for a hydraulic dysfunction (constraining pipes)

Fig. 5. Horizons for the evaluation of the hydraulic performance in the context of CC

Fig. 6. Identified constraining pipes for HDsf caused by Event 1 at the first horizon (H_1) in Network A

Fig. S-1. Proportion of total length constraining pipes for the six events and over the six horizons for Networks A (a) and B (b)

Fig. S-2. Identified constraining pipes (in red) for the first and the sixth horizons using Event 2 for Network A

Fig. S-3. Identified constraining pipes (in red) for the first and the sixth horizons using Event 3 for Network B

SUPPLEMENTARY INFORMATION

S.1 REVIEW OF PREVIOUS STUDIES EVALUATING THE IMPACT OF CC ON THE HYDRAULIC PERFORMANCE OF SEWER NETWORKS USING HH MODELS

The aim of this review is to show the diversity of HH models and CC projections that can be used. In several of these studies, conducted particularly in Europe, the MOUSE model (a component of the upgraded version MIKE URBAN; DHI, 2013) was used to evaluate the hydraulic performance of several sewer systems in relation to CC (Berggren *et al.*, 2014; Olsson *et al.*, 2013, 2009; Semadeni-Davies *et al.*, 2008). In these studies, the CC impact was assessed by adjusting rainfall intensity according to the season, and particularly according to the predicted results of different climate models conducted with several greenhouse gas (GHG) emission scenarios. Berggren *et al.* (2014), for example, used two distinct methods to obtain future rainfall intensities. The first is to apply a constant adjustment factor, derived from climate model results, to the intensity of the entire rainfall (design storm). The second is based on the delta change (DC) approach that estimates a distribution of DC factors (DCFs), which are the ratios between some percentiles of the future rainfall intensity distribution and the same percentiles in the current climate for the same season (Olsson *et al.*, 2009). In Berggren *et al.* (2014), the distribution of DCFs was applied to observed time series to define future rainfall event series, from which intense single rainfall events were extracted. Olsson *et al.* (2013) increased the intensity of a 1 h to 10-year return period design storm (by 23.6% between the 10th and 40th minutes and by 22.6% for the rest of the rain) to obtain a future rain event (horizon 2071-2100). The HH simulations of the network under future conditions were subsequently carried out using the MOUSE model with this modified design storm. These authors showed large deficiencies of the studied sewer pipes (located in Arvika, Sweden) in a future climate. Previously, for the sewer system of Kalmar (Sweden), Olsson *et al.* (2009) reported an increase of approximately 45% in the number of surface flooding events caused by the increase in intense precipitation intensities (20% and 30% in the summer and 50% to 60% in the autumn for the SRES-A2 scenario) by the end of the 21st century. These authors adjusted a continuous time series of precipitation, observed between 1991 and 2004, using the DC method.

Also in Sweden, Berggren *et al.* (2012) simulated the hydraulics and hydrology of a suburban sewer drainage system using the MIKE URBAN model. To this end, future rainfall series were created from observed rainfall series using the DC method. This analysis demonstrated that the number, frequency, and duration of floods and sewer backups should increase significantly in a future climate for the studied area.

The SWMM model was used to assess and predict the hydraulic performance of North American, European, and Asian urban sewer systems in different studies (Mikovits *et al.,* 2017; Kang *et al.*, 2016; Kirshen *et al*., 2015; Huong and Pathirana, 2013; Kleidorfer *et al.*, 2009; Denault *et al.*, 2006; Watt *et al.*, 2003; Waters *et al.*, 2003; Niemczynowicz, 1989). Mikovits *et al.* (2017) evaluated, with SWMM, the combined impact of urban development and CC on flooding volumes from a combined sewer network in Innsbruck, Austria. They showed that the impact of CC, i.e., more-intense heavy precipitation during summer, could be either compensated or amplified by urban development, depending on the spatial distribution of urban growth. For this evaluation, they used design rainfalls of various durations and return periods, which were modified using an empirical statistical downscaling method to produce future conditions over four GHG emission scenarios. Kirshen *et al.* (2015) applied SWMM to compute flooding volumes for the 3-month, 10-year, and 100-year design storms in Sommerville, U.S., for three time horizons: 2011, 2040, and 2070. The future design rainfalls were those developed by Powell (2008) for the case study area, applying a relative change factor to the intensities of historical design storms; these factors were derived from the outputs of 20 global climate models using two GHG emission scenarios.

Dale *et al.* (2017) applied the InfoWorks HH model (Innovyze, 2018) to four sewer networks in the U.K. They used as inputs to these models critical design storms, which were modified by applying percentages of change to rainfall depth to represent future climate. These percentages of change were computed by combining the results of two methods. The first one is based on climate analogues, in which UKCP09 CC projections (Murphy *et al.*, 2009) were used to identify the future mean summer temperature for the four study sites in 2030, 2050, and 2080. These temperatures were then used to select European cities (named contemporary climatological analogs) with similar mean summer temperatures in the current climate. Rainfall for 2- to 30-year return periods, for various durations, were computed using observed rainfall series in these contemporary analogs, and those were assumed to represent the future climate in the four studied cities. The second one compares rainfall intensities associated with various return periods, for the current and future climates, as computed with hourly precipitation data simulated during the very high-resolution (1.5-km grid boxes) CONVEX Project climate model experiment. For the four U.K. study sites, Dale *et al.* (2017) computed increases varying from 11% to 113% in sewer flooding volumes, which are higher than the increases in rainfall (7% to 50%), as well as increases in the number, frequency, and volume of combined sewer overflows.

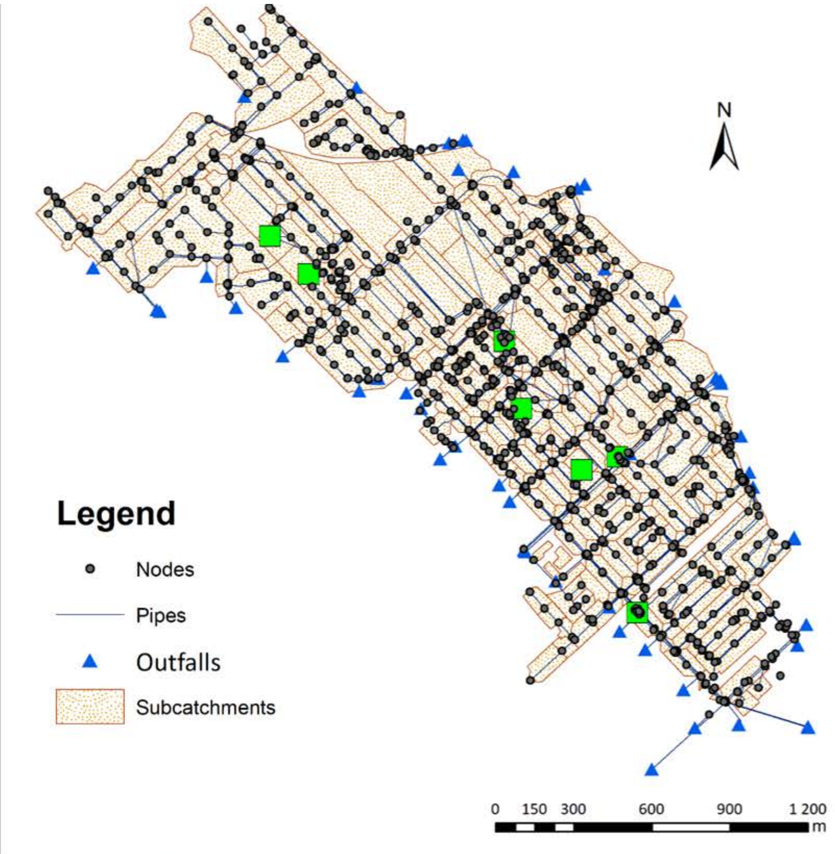
N
Legend
Nodes
Pipes
Outfalls
Subcatchments
0 150 300 600 900 1 200
m

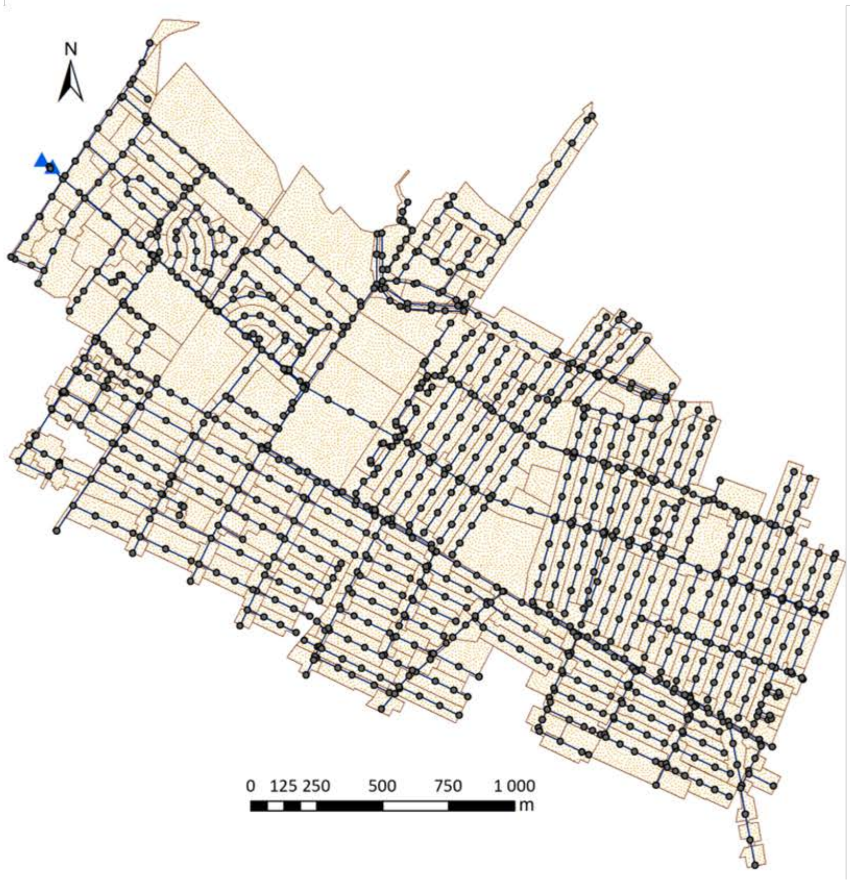
N
0 125 250 500 750 1 000
m

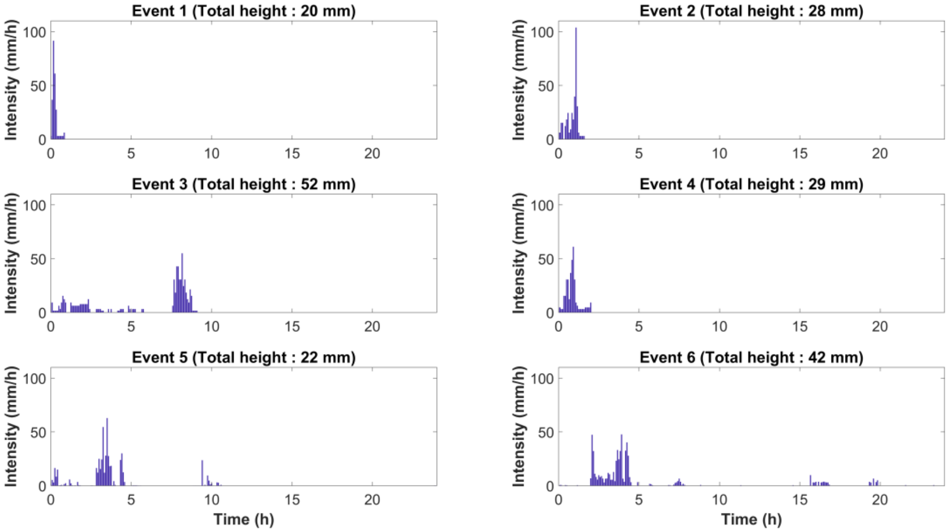
Event 1 (Total height : 20 mm)
Event 2 (Total height : 28 mm)
Event 3 (Total height : 52 mm)
Event 4 (Total height : 29 mm)
Event 5 (Total height : 22 mm)
Event 6 (Total height : 42 mm)
Intensity (mm/h)
0
50
100
0
5
10
15
20
Time (h)

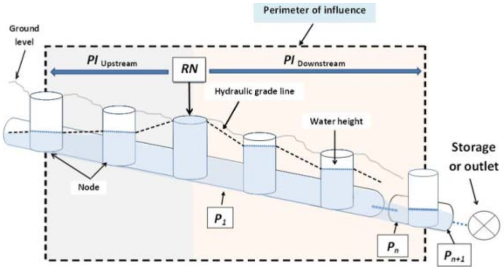
Perimeter of influence
Ground level
PI Upstream
RN
PI Downstream
Hydraulic grade line
Water height
Storage or outlet
Node
P1
Pn
Pn+1

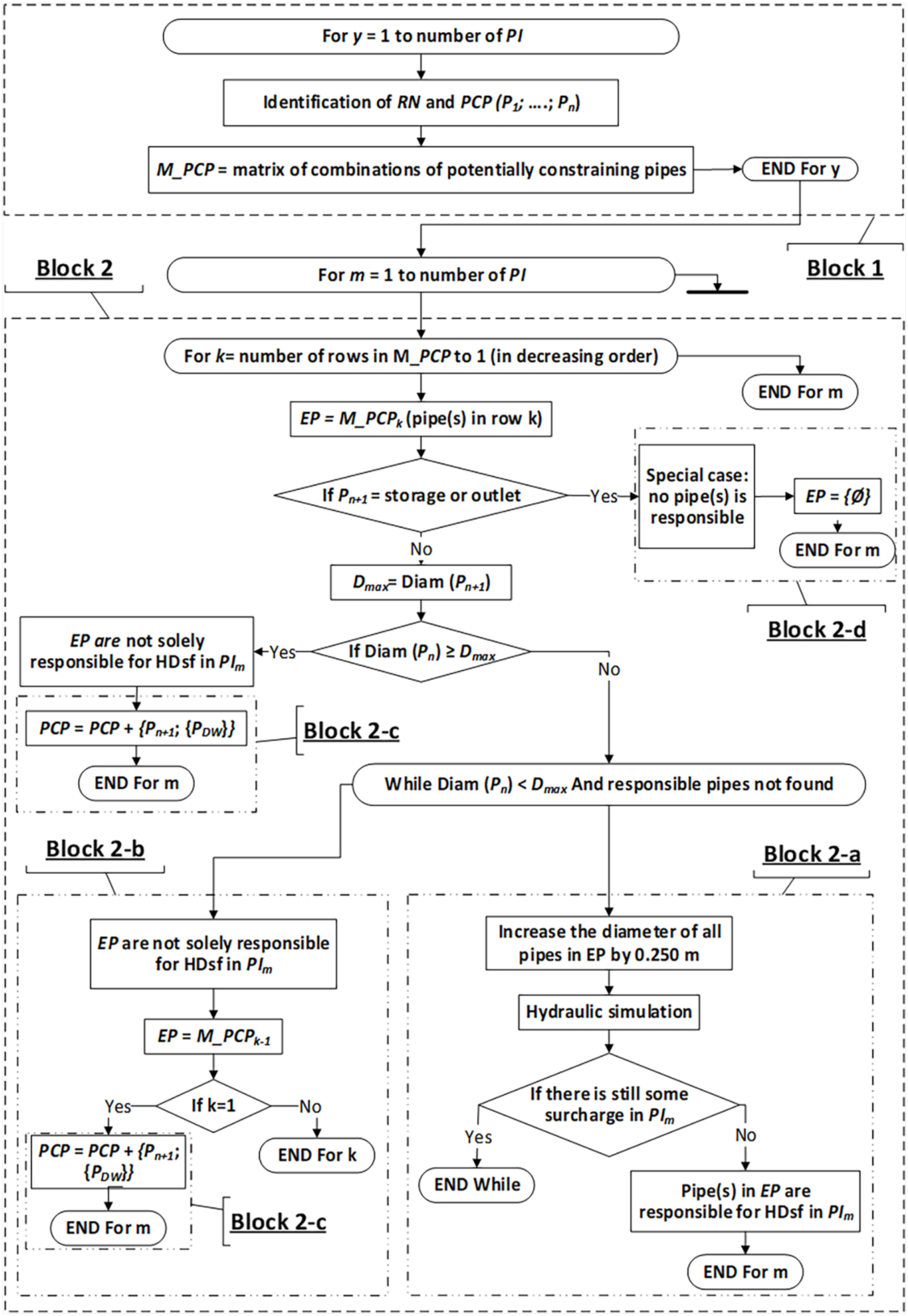
For y = 1 to number of PI
Identification of RN and PCP (P1; ….; Pn)
M_PCP = matrix of combinations of potentially constraining pipes
END For y
Block 1
Block 2
For m = 1 to number of PI
For k= number of rows in M_PCP to 1 (in decreasing order)
END For m
EP = M_PCPk (pipe(s) in row k)
If Pn+1 = storage or outlet
Yes
Special case: no pipe(s) is responsible
EP = {Ø}
END For m
Block 2-d
No
Dmax= Diam (Pn+1)
If Diam (Pn) ≥ Dmax
Yes
EP are not solely responsible for HDsf in PIm
No
PCP = PCP + {Pn+1; {PDW}}
Block 2-c
END For m
While Diam (Pn) < Dmax And responsible pipes not found
Block 2-b
Block 2-a
EP are not solely responsible for HDsf in PIm
EP = M_PCPk-1
If k=1
Yes
No
PCP = PCP + {Pn+1; {PDW}}
END For k
END For m
Block 2-c
Increase the diameter of all pipes in EP by 0.250 m
Hydraulic simulation
If there is still some surcharge in PIm
Yes
No
END While
Pipe(s) in EP are responsible for HDsf in PIm
END For m

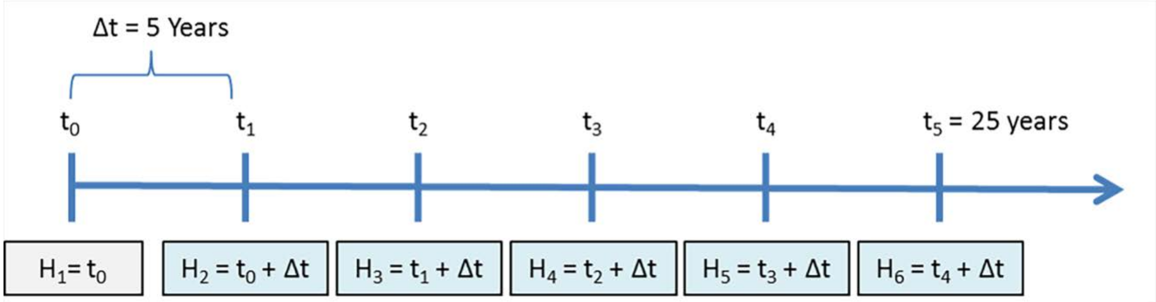
Δt = 5 Years
t_0
t_1
t_2
t_3
t_4
t_5 = 25 years
$H_1 = t_0$
$H_2 = t_0 + \Delta t$
$H_3 = t_1 + \Delta t$
$H_4 = t_2 + \Delta t$
$H_5 = t_3 + \Delta t$
$H_6 = t_4 + \Delta t$

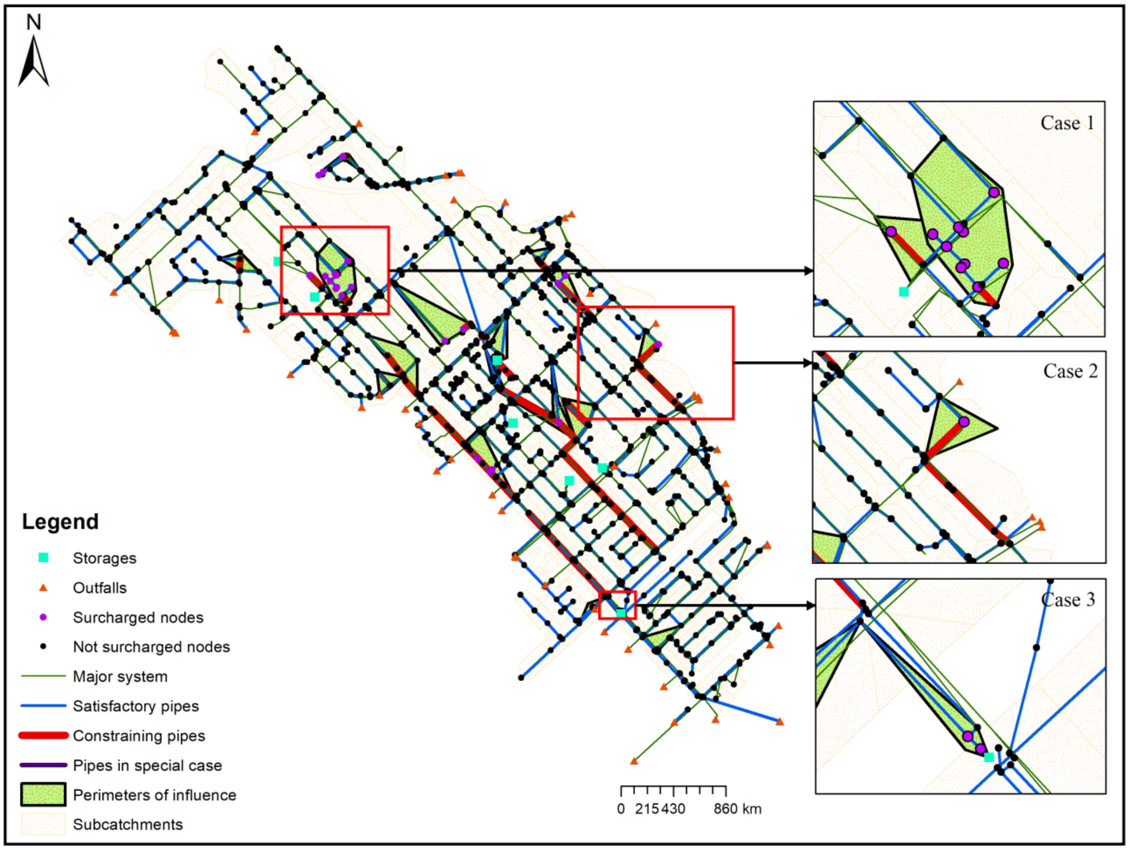
N
Case 1
Case 2
Case 3
Legend
Storages
Outfalls
Surcharged nodes
Not surcharged nodes
Major system
Satisfactory pipes
Constraining pipes
Pipes in special case
Perimeters of influence
Subcatchments
0 215 430 860 km

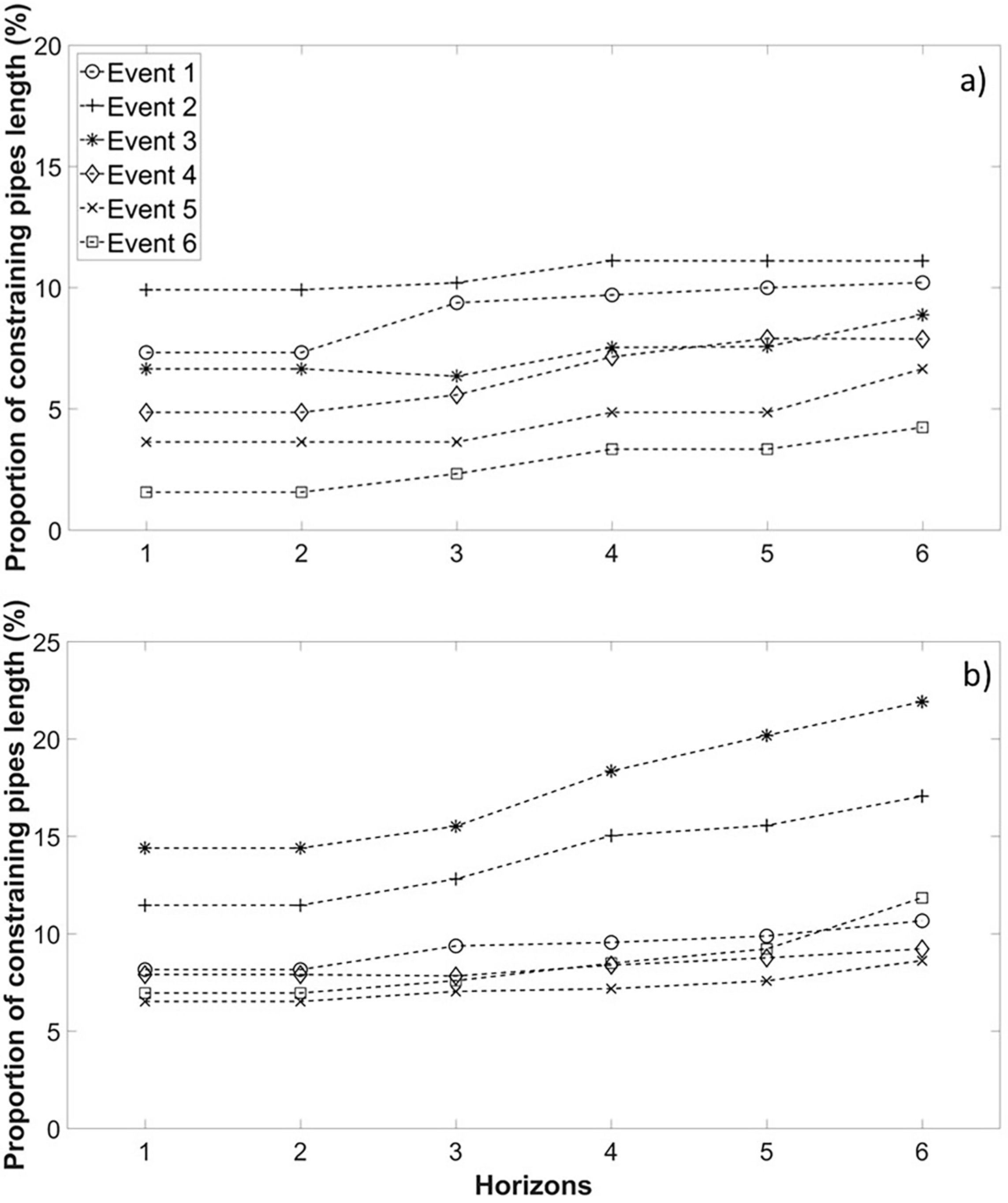
a)
Event 1
Event 2
Event 3
Event 4
Event 5
Event 6
Proportion of constraining pipes length (%)
0
5
10
15
20
1
2
3
4
5
6
b)
Proportion of constraining pipes length (%)
0
5
10
15
20
25
1
2
3
4
5
6
Horizons

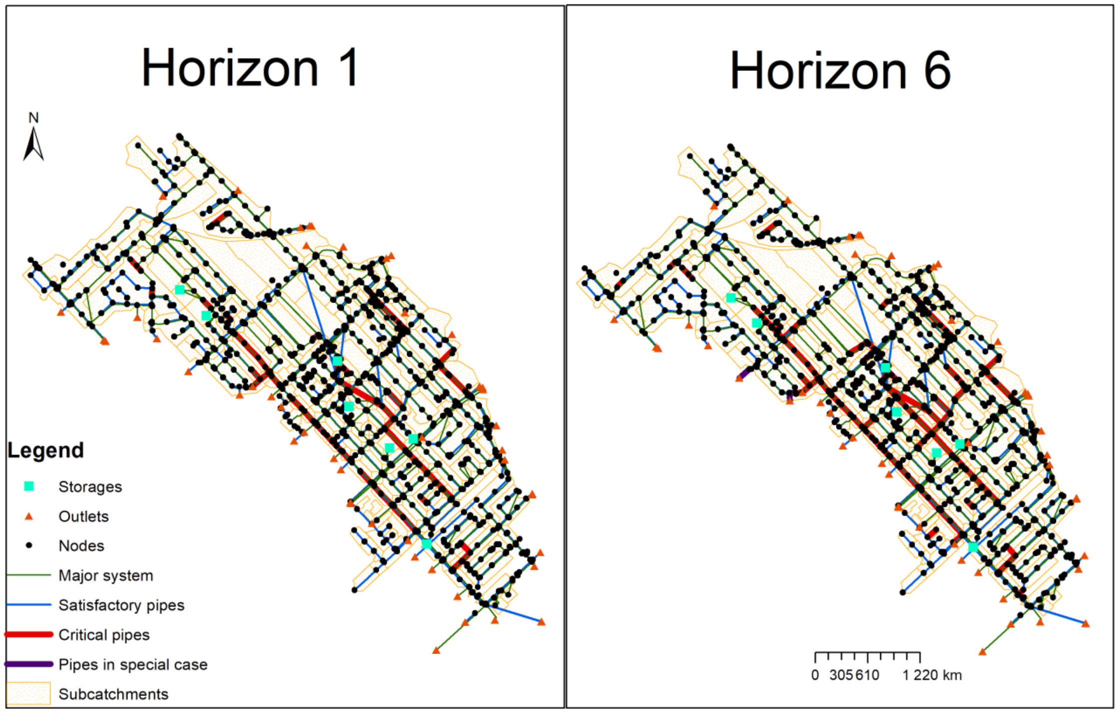
Horizon 1
Horizon 6
N
Legend
Storages
Outlets
Nodes
Major system
Satisfactory pipes
Critical pipes
Pipes in special case
Subcatchments
0 305 610 1 220 km

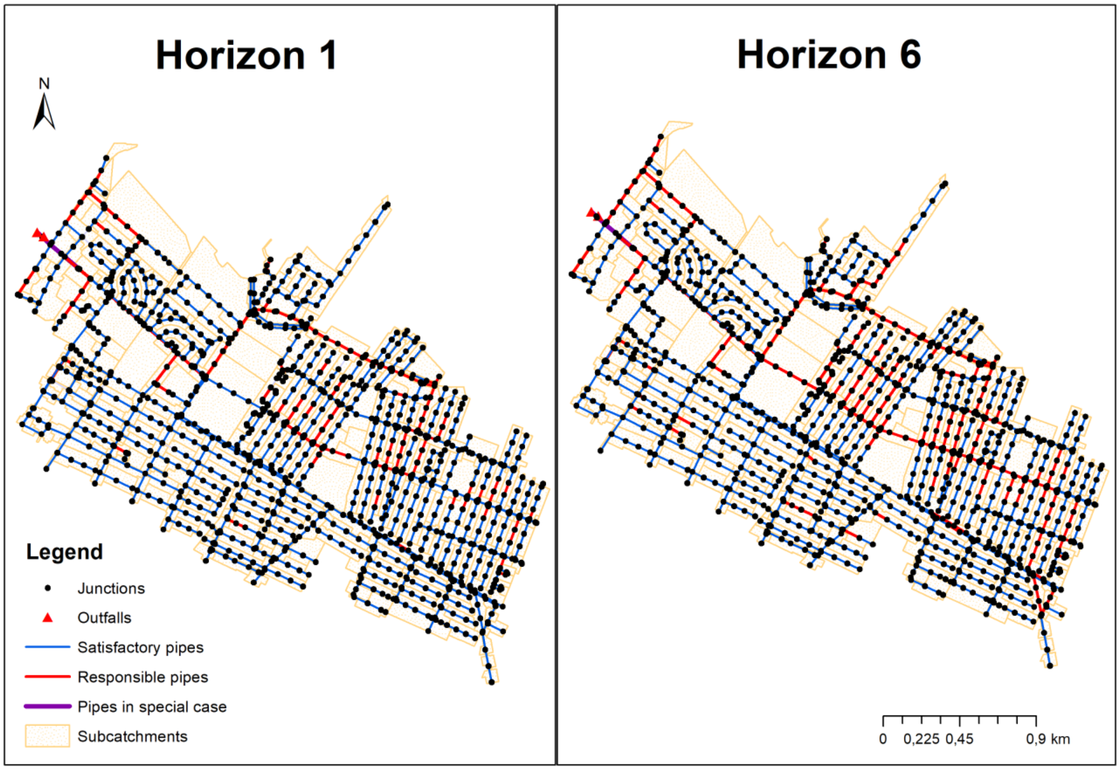
Horizon 1
Horizon 6
N
Legend
Junctions
Outfalls
Satisfactory pipes
Responsible pipes
Pipes in special case
Subcatchments
0
0,225
0,45
0,9 km